INFLUENCE OF ARCHING MECHANISM IN MASONRY WALLS STRENGTHENED WITH FRP LAMINATES

Nestore Galati, University of Missouri–Rolla, Rolla, MO

J. Gustavo Tumialan, University of Missouri–Rolla, Rolla, MO

Antonio Nanni, University of Missouri–Rolla, Rolla, MO

Antonio La Tegola, University of Lecce, Italy

Abstract

Fiber reinforced polymer (FRP) laminates have been proven to notably increase the flexural capacity of unreinforced masonry (URM) walls. This assertion is true in the case of walls that can be treated as simply supported (i.e. walls exhibiting large slenderness ratios). For walls with low slenderness ratios and that are built between rigid supports, when the out-of-plane deflection increases, the wall is restrained from free rotation at its ends. This action induces an in-plane compressive force, which, depending on the degree of support fixity, can increase several times the wall capacity. This mechanism is known as arching. Due to arching, the increase of capacity in walls strengthened with FRP laminates may be considerably less than expected. This paper presents the experimental results of masonry specimens confined by two rigid supports, simulating upper and lower floor beams, subjected to out-of-plane loading. Experimental results show that the contribution of FRP to the wall capacity is less than in the case of simply supported conditions. An analytical method is used for determining the capacity of masonry walls strengthened with FRP laminates considering the arching mechanism. The method analyzes infill walls that span between two rigid supports. The method shows good agreement with the experimental results and allows for appropriate design.

Introduction

Masonry walls may be subjected to out-of-plane loads caused by high wind pressures or earthquakes. Externally bonded fiber reinforced polymer (FRP) laminates or near-surface-mounted (NSM) FRP bars have been successfully used to increase the flexural capacity of masonry members subject to out-of-plane loads (Ehsani et. al., 1999, Hamilton et. al. 1999, Tumialan et. al., 2002).

The load-resisting mechanisms for FRP strengthened unreinforced masonry (URM) walls depend on the tensile strength of masonry, in-plane compressive strength, boundary conditions, slenderness ratio (height/thickness), and material and bond properties of the FRP. When a wall is built between supports that restrain the outward movement, membrane compressive forces in the plane of the wall, accompanied by shear forces at the supports are induced as the wall bends.

The in-plane compression forces can delay cracking. After cracking, a so-called arching action can be observed. Due to this action, the capacity of the wall can be much larger than that computed assuming simply supported conditions. Analysis has shown that the induced forces can increase the cracking load by a factor of about 2.5 if the end supports are completely rigid (L.R. Baker, 1978; A.W. Hendry, 1981). Experimental works (Tumialan et. Al. 2001) have shown that the resultant force between the out-of-plane load and the induced membrane force could cause the crushing of the masonry units at

the boundary regions. In this case, the application of the FRP did not exhibit the same effectiveness as in the case of walls having simply supported conditions. This paper presents the experimental results of a group of ten walls having a slenderness ratio equal to 12, confined by two rigid supports. A comparison between the experimental and analytical values of out-of-plane capacity is also presented.

Experimental Program

As shown in Table 1, ten specimens were built in order to investigate the FRP effectiveness in walls exhibiting arching action. Five specimens were built with concrete blocks. The remaining five were built with clay masonry bricks. The nominal dimensions of these walls were 1.22 m (48 in.) by 0.61 m (24 in.); their overall thickness was 95 mm (3 ¾ in.) for clay specimens and 92 mm (3 ⅝ in.) for concrete specimens, (Figure1). To study modes of failure, different amounts of glass FRP (GFRP) reinforcement were applied to the wall surface and expressed as a function of the balanced reinforced ratio, ρ_b. The balanced condition occurs when the compressive failure of the masonry is reached at the same time that the FRP laminate fails in tension. Two different surface preparation methods (with or without putty filler) were used. The surface preparation of all the masonry specimens built with clay units included the use of putty.

This was because the clay brick wall surfaces exhibited more unevenness than those with concrete blocks. The two series of walls were coded: CLx and COx. The first two characters in the code represent the type of masonry used, "CO" for concrete masonry and "CL" for clay masonry. The last character is a number that indicates the width of the GFRP strip in inches (one strip per specimen). Thus, CL3 is a clay masonry wall, strengthened with a GFRP laminate having a width of 75 mm (5in.). The specimens CL0 and CO0 are the control walls for clay and concrete masonry units respectively. In every case, the length of the FRP strips was 1170 mm (46 in.); in this manner the laminate would not touch the roller supports used for testing.

Table 1. Test Matrix

Specimen	Masonry Type	Thickness mm (in)	GFRP width mm (in)	r_b (%)	h/t ratio
CL0	Clay	95 (3 ¾)	-	-	12.8
CL3	Clay	95 (3 ¾)	76.2 (3)	43	12.8
CL5	Clay	95 (3 ¾)	127.0 (5)	72	12.8
CL7	Clay	95 (3 ¾)	177.8 (7)	100	12.8
CL9	Clay	95 (3 ¾)	228.6 (9)	130	12.8
CO0	Concrete	92 (3 ⅝)	-	-	13.2
CO3	Concrete	92 (3 ⅝)	76.2 (3)	100	13.2
CO5	Concrete	92 (3 ⅝)	127.0 (5)	167	13.2
CO7	Concrete	92 (3 ⅝)	177.8 (7)	233	13.2
CO9	Concrete	92 (3 ⅝)	228.6 (9)	300	13.2

Note: ρ_b = balanced condition; h=height of the wall; t=thickness of the wall

For each specimen, a GFRP laminate was installed only on one side of the wall along the longitudinal axis. For the installation, the manual lay-up technique was followed.

Five strain gages (uniformly distributed and in correspondence of the bed joints where crushing is expected) were applied on the GFRP laminate (Figure 1) to monitor the tensile strain distribution along the laminate during the test.

Tests were performed to characterize the engineering properties of the materials used in this investigation. The average compressive strengths of concrete and clay masonry obtained from testing of prisms (ASTM C1314) were 10.5 MPa (1520 psi) and 17.1 MPa (2480 psi), respectively. Standard mortar specimens were tested according to ASTM C109. An average value of 7.6 MPa (1100 psi) at an age of 28 days was found; therefore, the mortar can be classified as Type N.

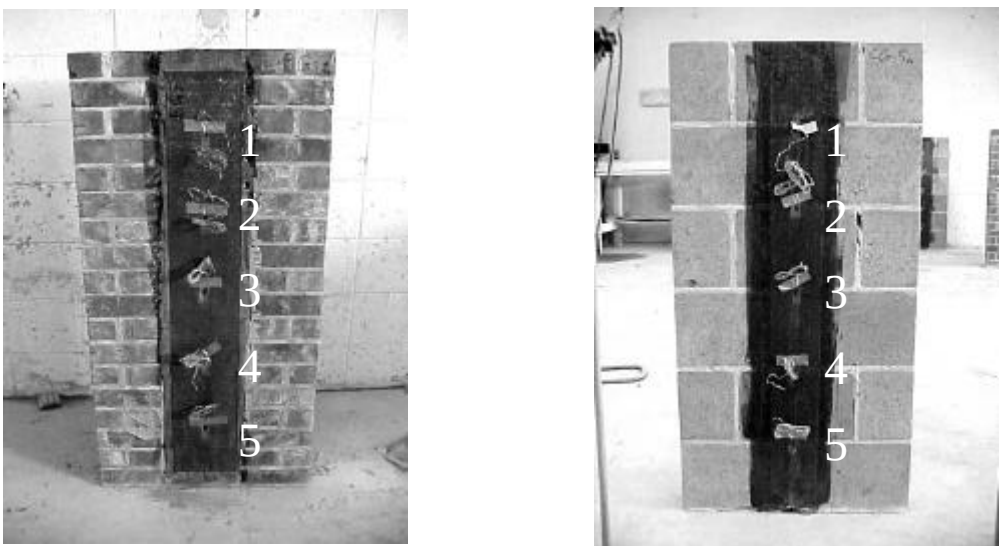

Figure 1. Test Specimens and Strain Gage Locations

Tensile tests were performed on FRP laminates to determine their engineering properties. The test results showed that the tensile strength of GFRP was 1690 MPa (245 ksi) and the modulus of elasticity was 92.9 GPa (13.46 msi).

Test Setup

To reproduce the real boundary conditions when the wall is restrained inside a reinforced concrete (RC) frame, and to separate the two reaction forces (shear and in-plane load at the support), four reinforced concrete members were used. The bottom members provided the vertical reaction (See Figure 2). The top member resisted the horizontal load, created by the arching effect of the wall. High strength steel rods were used to connect these members to the steel test frame.

The masonry walls were tested under four-points bending. Loads were applied by 50.8 x 609.6 x 12.7 mm (2 x 24 x ½ in.) steel plates to the external face of the wall (figure 2). Their distance was 101.6 mm (4 in.) from the midspan. The loads were generated by means of a 12 ton hydraulic jack reacting against a steel frame. Linear Variable Displacement Transducers (LVDTs) were positioned in the middle of the walls to measure the midspan deflection during the tests. Two load cells were used to record the in-plane (load cell 2) and the out-of-plane (load cell 1) loads. A horizontal load of 2.9 kN/m (200 lb/ft) was applied before testing to hold the walls in place. This load was selected in accordance with the Masonry Joint Standards Committee (MSJC, 1999) recommendations, which specify that level of load as the limit between non-loadbearing and loadbearing walls.

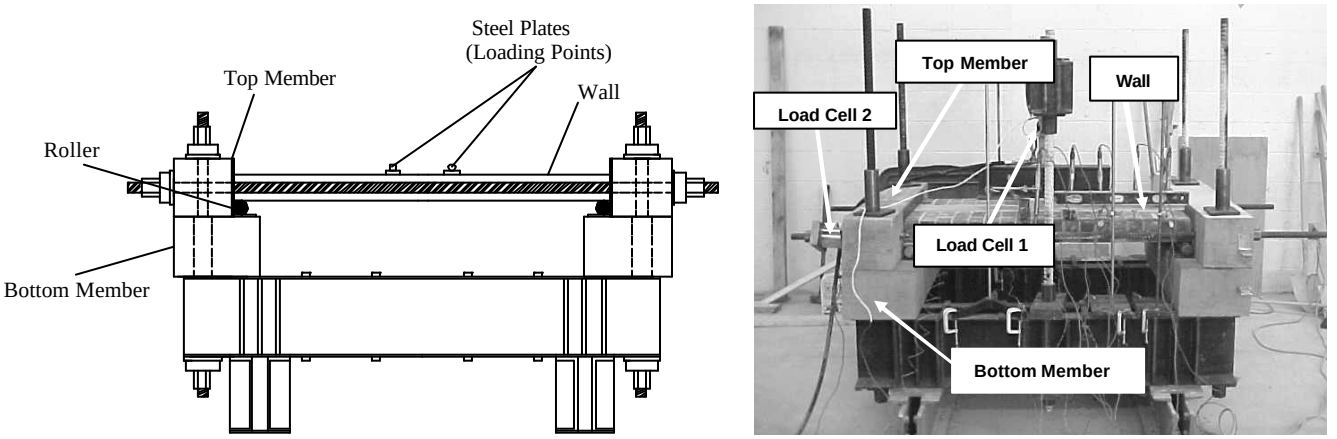

Figure 2. Test Setup Scheme

Test Results

Three different modes of failure were observed:

- **Flexural Failure:** after developing flexural cracks primarily located at the mortar joints, a wall failed by either rupture of the FRP laminate or masonry crushing depending on the reinforcement ratio, ρ, and arching effect.
- **Crushing of the masonry at the supports**: this is the most common mode of failure in walls in which arching mechanism occurs. This kind of failure is due to the resultant force from shear and the in-plane forces at the supports.
- **Shear Failure**: cracking started with a development of fine vertical cracks at the maximum bending region. Only flexural-shear failure was observed. The sliding shear was not observed because of the in-plane force at the supports.

In the control specimens and in specimens CL3, CL5, CO3 and CO5 crushing of the masonry units at the boundary regions was observed. For specimens CL7, CO7, CL9 and CO9 failure occurred due to the shear. Figure 3 shows a series of pictures illustrating the various modes of failure.

Tests results in terms of ultimate load and maximum midspan deflection are summarized in Table 2. For the midspan deflection, the average value of the two LVDTs was used unless noted.

Results Discussion

Figure 4 illustrates the out-of-plane load versus the mid-height deflection obtained for all specimens. For the clay masonry specimens (Figure 4a), a remarkable increment of flexural capacity compared to the control wall can be observed for all reinforced specimens. This increment may be overly optimistic because the arching mechanism was not completely developed in the control specimen due to set-up difficulties. It can observed from Figure 4a that the different amounts of reinforcement do not dramatically influence the ultimate load. Higher reinforcement can only increase the stiffness and reduce deflection. By increasing the amount of reinforcement a drop in ductility was observed.

The results obtained in the case of the concrete blocks were similar to the ones obtained in the case of the clay bricks (see Figure 4b) even though the performance of the control specimen was closer to that of the reinforced ones.

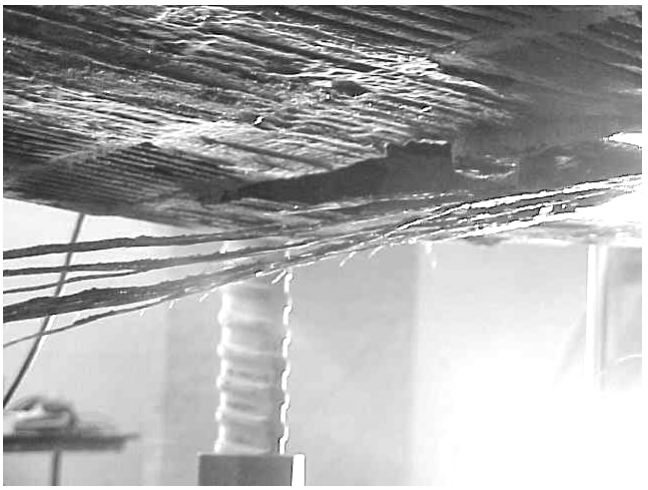

(a) Fiber Rupture (CL3)

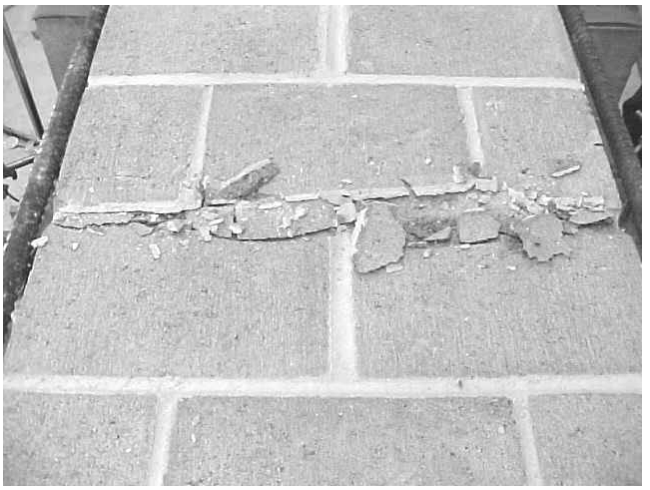

(b) Crushing of Units at Midspan (CO0)

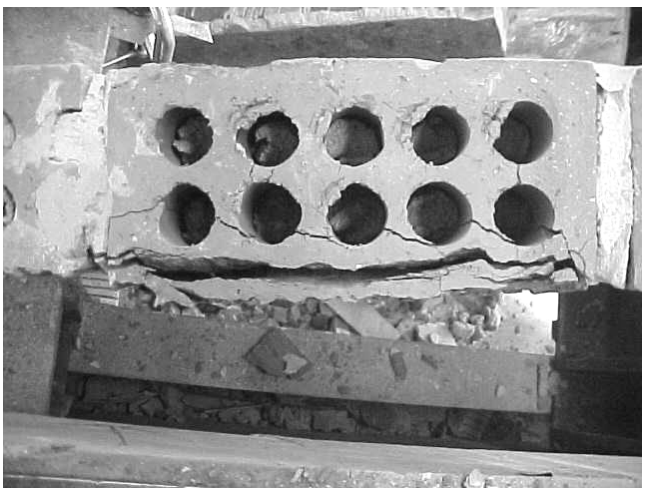

(c) Crushing of Units at Support (CL5)

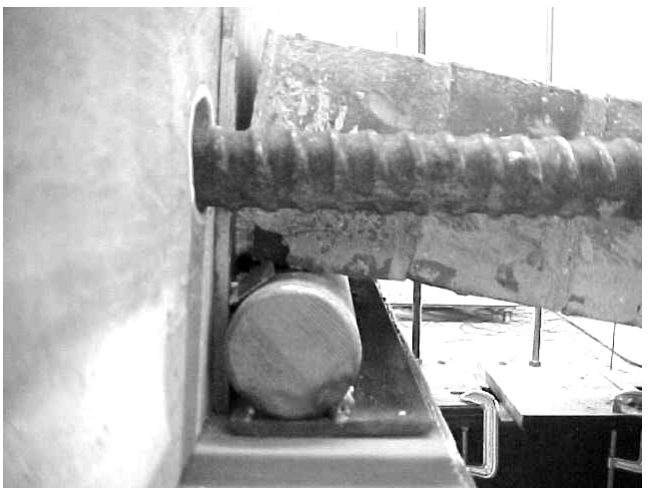

(d) Crushing of Units at Support (CL5)

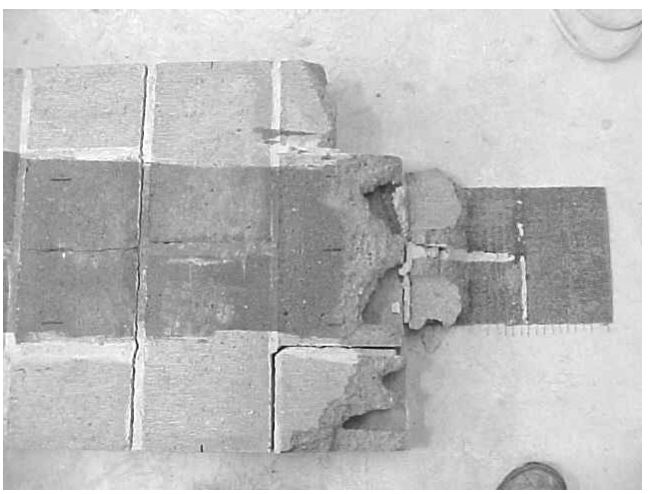

(e) Shear Failure (CO9)

(f) Shear Failure (CL9)

Figure 3. Failure of the Specimens

Table 2. Test Results

Specimen	Out-of-Plane Load (kN)	In-Plane Load (kN)	Midspan Deflection [mm]	Mode of Failure
CL0	21.3	57.8	30.1(*)	Crushing of Masonry Units
CL3	52.2	115.6	31.7	Fiber Rupture
CL5	45.6	101.4	28.9(*)	Crushing of Masonry Units
CL7	54.9	97.9	24.1	Masonry Shear
CL9	53.1	80.9	18.1	Masonry Shear
CO0	22.4	83.6	31.1(*)	Crushing of Masonry Units
CO3	29.0	82.7	26.5	Crushing of Masonry Units
CO5	27.1	58.7	18.1	Crushing of Masonry Units
CO7	33.1	58.7	20.7	Masonry Shear
CO9	34.7	38.3	21.6	Masonry Shear

Note: 1 mm = 0.03937 in.; 1 KN = 0.2248 kips (*):one LVDT

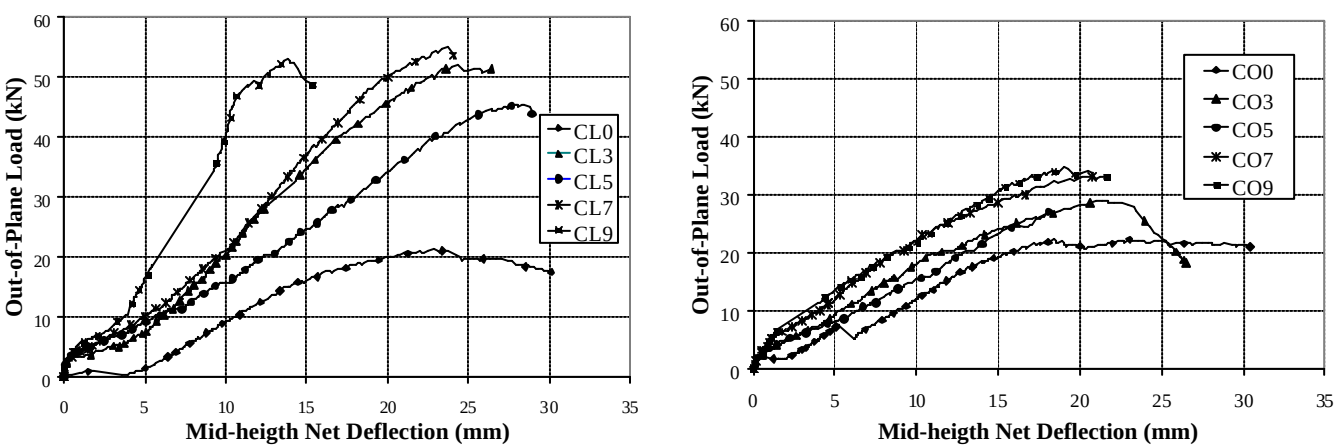

(a) Clay Masonry (b) Concrete Masonry

Figure 4. Load vs. Mid-height Deflection

By analyzing the experimental data, it is observed that when the first crack appeared in the walls, the in-plane restraining force suddenly increased. This can be referred to as the arching action. By

plotting the out-of-plane load versus the in-plane load, it can be observed that the in-plane load remains practically constant until the first crack appears in the specimens (see Figure 5) and then grows almost linearly.

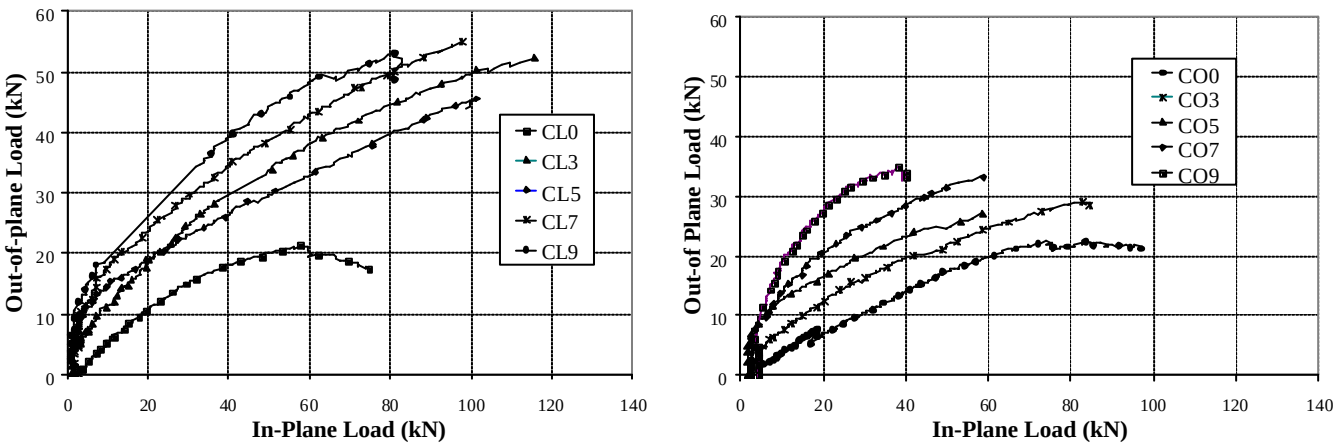

(a) Clay Masonry (b) Concrete Masonry

Figure 5. In-Plane Load vs. Out-of-Plane Load

By increasing the amount of FRP, due to the reduction of the displacement, the in-plane load decreased. The same trend can be observed by analyzing the maximum in-plane/out-of-plane load ratio as a function of the FRP width (Figure 6). The test results show a consistent pattern. The in-plane/out-of-plane load ratio decreases linearly when the FRP amount increases.

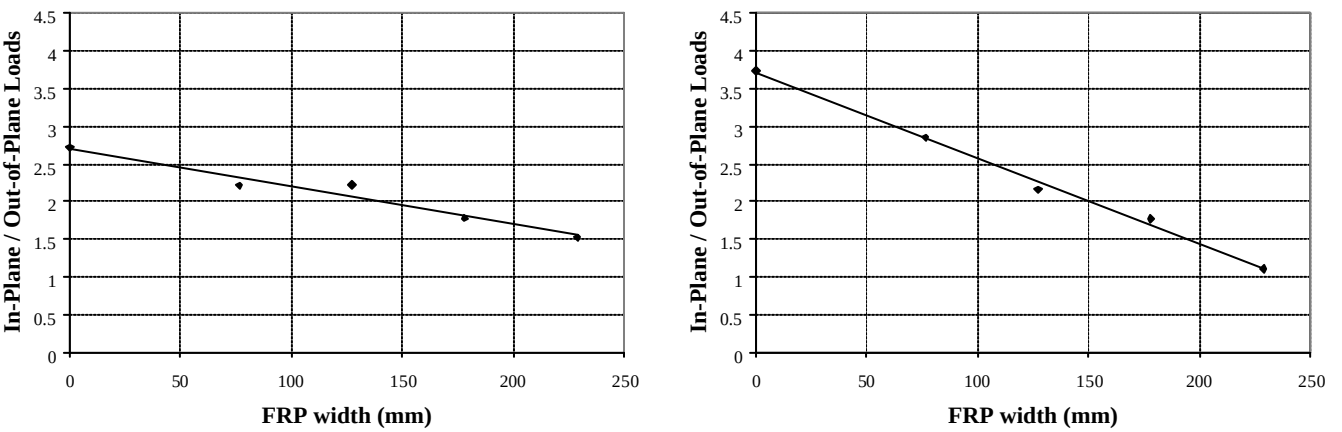

(a) Clay Masonry (b) Concrete Masonry

Figure 6. In-Plane/Out-of-Plane Load Ratio as a Function of FRP Width

Figure 7 illustrates a comparison between the load-deflection curves obtained in the case of simply supported walls (Tumialan et al., 2002) and walls with the end restrained. A significant influence of the boundary conditions in the wall behavior is observed.

If the wall behaves as a simply supported element (i.e. large slenderness ratio or upper end is not restrained), the FRP reinforcement is very effective since the wall is in pure flexure and the crack openings are bridged by the reinforcement. In the case of the simply-supported specimens, the URM wall collapsed when the vertical load was about 3.1 kN (0.7 kips). Figure 7 shows that the increase in

the ultimate load for walls strengthened with 75 mm (3 in.) and 125 mm (5 in.) wide GFRP laminates were about 175 and 325%, respectively. If the wall is restrained (i.e. arching mechanism is observed) the same effectiveness of the FRP reinforcement is not observed because crushing of the masonry units at the boundary regions controls the wall behavior. In this case, the increase in the out-of-plane capacity for strengthened specimens with 75 mm (3 in.) and 125 mm (5 in.) wide GFRP laminates was about 25%.

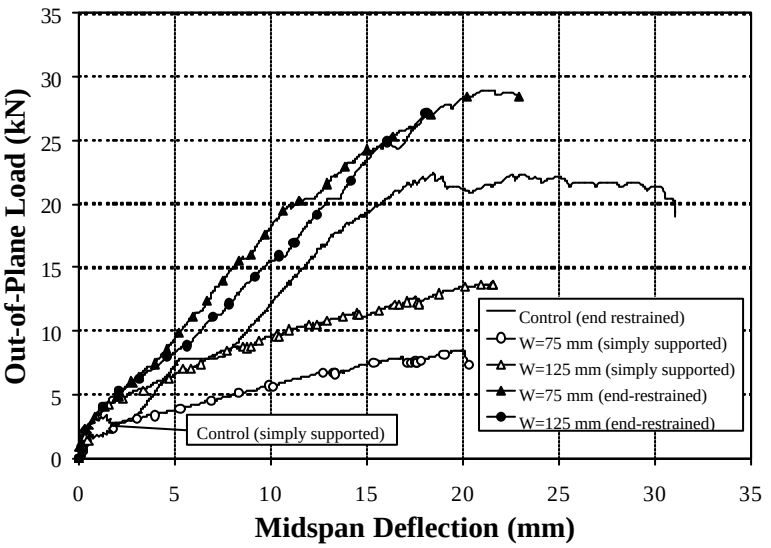

Figure 7. Comparison between Simply Supported and End-Restrained Walls

Analytical Study

The experimental results have been compared with the analytical result obtained using a model developed by the same authors (Tumialan et. al., 2001). Using this model it is possible to determine the out-of-plane and in-plane loads, mid-height deflection, and rotations at the supports that both unreinforced and externally strengthened walls can resist. In the present analytical formulation, the wall is idealized as a unit strip subjected to a concentrated load applied normal to its plane. This model can be extended to distributed loads. The model takes into account the clamping forces in the supports, originated by arching action, which leads to increasing the out-of-plane resistance. Previous researchers (Fricke, 1992, Angel et al., 1994) have found this resistance to be many times greater than the one predicted by conventional theories that do not consider post-cracking mechanisms.

To formulate the analytical model, it is assumed that constituent materials are linearly elastic up to failure. For the case of masonry, a previous research study has demonstrated that consideration of a triangular stress distribution is adequate for arching mechanisms (Angel et al., 1994). It is also assumed that the wall is only cracked at mid-height, and that the two resulting segments can rotate as rigid bodies about the supports as illustrated in Figure 8. As a limit state, crushing of masonry at the boundary regions or flexural failure (i.e. rupture of fiber or crushing of masonry) is considered.

The forces F_V and F_H represent the in-plane reaction and the shear force at the support respectively. The resultant force from F_V and F_H causes, in many cases, the crushing of the masonry units at the support. The aforementioned analytical model fits very well with the experimental results (Table 3).

The discrepancy between the analytical and the experimental results for the CL0 specimen was caused by problems occurred during the test. The model indicates that the predicted load for specimen CL3 was the limit between crushing of masonry at the supports and rupture of FRP. The latter was attained experimentally.

Shear failure was registered for specimens CL7, CL9, CO7, and CO9. The comparison between the experimental and predicted loads for these specimens suggests that crushing of the masonry units at the boundary regions was close to occur.

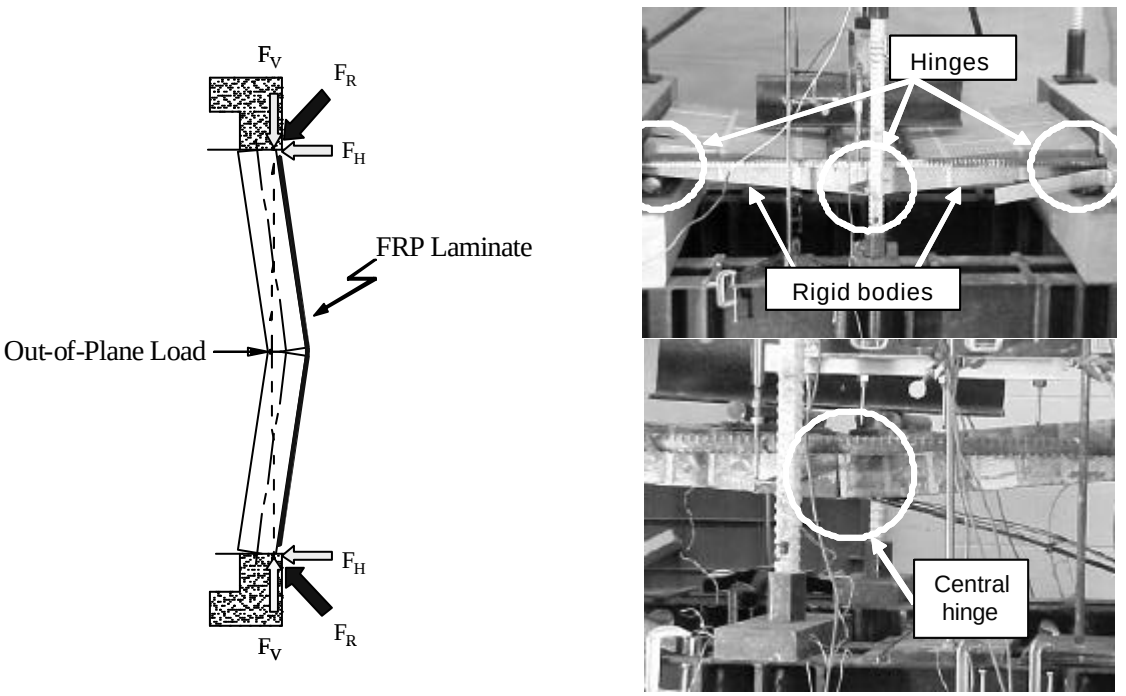

Figure 8. Out-of-Plane Mechanism of Failure

Table 3. Comparison between Theoretical and Analytical Out-of-Plane Loads

Specimen	FRP width (mm)	Experimental Load (kN)	Predicted Load (kN)	Percentage of Error (%)
CL0	0	21.3	44.1	107
CL3	75	52.2	51.0[(1)]	2
CL5	125	45.6	54.8	20
CL7	175	55.0	58.1[(2)]	5
CL9	225	53.1	61.0[(2)]	15
CO0	0	22.4	24.0	7
CO3	75	29.0	29.4	1
CO5	125	27.1	32.0	18
CO7	175	33.1	34.5[(2]	4
CO9	225	34.7	36.5[(2)]	5

Note: 1 mm = 0.03937 in.; 1 KN = 0.2248 kips
[(1)] Specimen failed by FRP rupture
[(2)] Specimens failed by shear

Conclusions

The following conclusions can be drawn from this experimental program:

- A mechanism of failure that is not commonly considered for the analysis of FRP strengthened walls was studied. End-restrained walls exhibited an arching mechanism where crushing at the supports controlled the wall behavior. This mechanism of failure must be considered in the quantification of upgraded wall capacities to avoid overestimating the wall response.
- The analytical model used to determine the peak load and deflection of both unreinforced and strengthened walls shows good agreement with experimental results and can be easily modified to take into account distributed loads acting on the wall, and incorporated in design provisions.

Acknowledgements

The support of the National Science Foundation Industry/University Cooperative Research Center at the University of Missouri–Rolla and Rolla Technical Institute (RTI) are acknowledged. The authors would also like to thank Marco Casareto, Alessandro Oliveri, and Alessandro Romelli, UMR Visiting Scholars from the University of Genoa, Italy, for their assistance.

References

1. Angel, R., Abrams, D. P., Shapiro, D., Uzarski, J., and Webster, M. (1994). "Behavior of Reinforced Concrete Frames with Masonry Infills." Struct. Res. Ser. 589, Department of Civ. Engrg., University of Illinois at Urbana-Champaign, IL.
2. Baker L. R., (1978) " Precracking Behavior of Laterally Loaded Brickwork Panels with In-Plane Restrains," in Proceedings of the British Ceramic Society, No. 27, pp. 129 -146.
3. Ehsani, M. R., Saadatmanesh, H., and Velazquez-Dimas, J. I. (1999). "Behavior of Retrofitted URM Walls Under Simulated Earthquake Loading." J. of Comp. for Const., ASCE, 3(8), 134-142.
4. Hamilton, H.R. III, Holberg, A., Caspersen, J., and Dolan, C. W. (1999). "Strengthening Concrete Masonry with Fiber Reinforced Polymers." 4th Int. Symp. on Fiber Reinf. Polymer (FRP) for Reinf. Conc. Struct., Baltimore, MD, 1103-1115.
5. Hendry A. W., (1981). "Structural Brickwork", pp. 128 and 141, The Macmillan Press Ltd., Landon.
6. Masonry Standards Joint Committee. (1999). "Building Code Requirements for Masonry Structures." ACI-530-99/ASCE 5-99/TMS 402-99, Detroit, MI, New York, NY, and Boulder, CO.
7. Tumialan J. G. (2001). "Strengthening of Masonry Structures with FRP Composites." Doctoral Dissertation, University of Missouri-Rolla, Rolla, MO
8. Tumialan, J. G., Galati, N., and Nanni, A., (2002). "Field Assessment Of URM Walls Strengthened With FRP Laminates", submitted to the Journal of Structural Engineering.
9. Tumialan, J. G., Galati, N., Namboorimadathil, S. M., and Nanni, A., (2002). "Strengthening of Masonry with FRP Bars" ICCI 2002, San Francisco, CA, June 10-12, 2002
10. Tumialan J.G., Morbin A., Micelli F. and Nanni A., (2002). "Flexural Strengthening of URM Walls with FRP Laminates," ICCI 2002, San Francisco, CA, June 10-12, 2002